Accepted Manuscript

Interface engineering in ferromagnetic high-thermal conductivity iron-diamond/metal composites for electric conversion applications

J.M. Molina, E. Louis

PII: S0925-8388(17)33756-8

DOI: 10.1016/j.jallcom.2017.11.010

Reference: JALCOM 43703

To appear in: *Journal of Alloys and Compounds*

Received Date: 24 July 2017

Revised Date: 31 October 2017

Accepted Date: 2 November 2017

Please cite this article as: J.M. Molina, E. Louis, Interface engineering in ferromagnetic high-thermal conductivity iron-diamond/metal composites for electric conversion applications, *Journal of Alloys and Compounds* (2017), doi: 10.1016/j.jallcom.2017.11.010.

Interface engineering in ferromagnetic high-thermal conductivity iron-diamond/metal composites for electric conversion applications

J.M. Molina[1,2,3 *] and E. Louis[1,3,4]

[1] Instituto Universitario de Materiales, Universidad de Alicante, Apdo 99, E-03080 Alicante, Spain
[2] Departamento de Química Inorgánica, Universidad de Alicante, Apdo 99, E-03080 Alicante, Spain
[3] Departamento de Física Aplicada, Universidad de Alicante, Apdo 99, E-03080 Alicante, Spain
[4] Unidad Asociada del Consejo Superior de Investigaciones Científicas, Universidad de Alicante, Apdo 99, E-03080 Alicante, Spain

* corresponding autor (e-mail: jmmj@ua.es)

Abstract

The objective of this work is to investigate whether any combination of metal and magnetic particles may fit the specifications of electric conversion applications, which require, among other properties, sufficiently high magnetic permeability and thermal conductance and a low (adjustable) thermal expansion coefficient. After having explored a wide variety of combinations, guided by both chemical and physical considerations, it was decided to investigate composites fabricated by gas pressure infiltration of Ag or Ag3wt%Si alloys into compacts of bimodal mixtures of diamond (high thermal conductivity) and iron particles (high magnetic permeability). Three average particle sizes of each component were used to fabricate the composites, namely, diamond particles of 230, 285 and 295 μm and iron particles of 30, 42 and 398 μm. In addition the volume fraction varied in the ranges 0.1-0.59 (diamond) and 0.12-0.43 (iron). In order to avoid alloying with the infiltrating metal and iron-diamond reaction, iron particles were coated with amorphous carbon. The results indicate that only composites containing a volume fraction of carbon-coated iron particles higher than 0.4 showed properties (a thermal conductance higher than 200 W/mK and a relative magnetic permeability above 0.3) within the range valid for electric conversion applications. Composites containing non-coated iron particles reached in almost all cases very low values of both properties.

1. Introduction

Some of the high-end applications in the field of electric conversion have reached their technological limits because of the impossibility of finding materials with acceptable ferromagnetic properties and, at the same time, capable to dissipate the excessive heat generated in their normal running [1-5]. Monolithic materials like carbon or steel have been traditionally used in the cores of the converter units.

However, their thermal conductivity is extremely low and cannot accomplish the future demands of power control, since overheating of the systems would pose problems for keeping the structural integrity of the whole equipment. There is, in consequence, a need to identify new developments of ferromagnetic materials with improved thermal conductivity.

Composite materials with ferromagnetic properties have been since long fabricated by incorporating ferromagnetic materials as finely divided inclusions (like iron powders or fibers [2,4], barium ferrites [4], strontium particles [6], flakes of Fe-Cr [7], SmCo5 [8], iron nitride [9], iron oxide [10], CoFe [11] and ferrites [12,13]) into different non-magnetic metal matrices (Zn-22Al, Cu-ZnAl, $Nb_{0.33}Cr_{0.67}$, silver and copper). These soft magnetic powder-based composites (FPC), often fabricated by the established procedures of powder packing and ulterior densification by liquid infiltration with an appropriate matrix, were firstly developed aiming to replace some steel parts, subjected to time-varying magnetic fields, in electromagnetic devices of high power converter units and electric motors [1-5]. However, this class of FPC composites likely have excessively low thermal conductivity, still far from being auspicious for proper heat dissipation.

Other family of FPC materials fabricated with iron or ferrite powders and polymeric matrices, do not accomplish the current needs of thermal management for the mentioned applications. Aiming to increase the thermal response of these composites, it was explored the route of embedding a mixture of a ferromagnetic powder and dispersed heat conductive particles (SiC, AlN, BN, BeO, etc.) in a polymeric matrix; these composites, however, did not either show promising properties [14,15].

The present work is addressed to develop new ferromagnetic-high thermal performance three-phase composite materials through another approach that consists of combining high thermally conductive diamond particles with iron powder in a bimodal filler architecture, subsequently consolidated with silver matrix by gas pressure infiltration. In order to make effective the high thermal conductivity of metal and diamond particles, interfacial engineering must be applied, with the aim of achieving the proper heat transfer between the different phases.

Silver has been selected as metal matrix for their high thermal conductivity. In contrast to aluminium, another non-ferromagnetic metal often selected as matrix for composite materials, pure silver does not react with diamond and, in consequence, the interfaces are weakly conductive. Additions of silicon into silver have proven to increase the thermal conductivity of silver/diamond composites [16]. Regarding the ferromagnetic filler, iron particles reacts with silver and silver-silicon alloys, forming inter-metallics

with poor thermal conductivity and low magnetic permeability. For this reason, along with the fact that iron, at temperatures of composites processing, may catalyse the transformation of diamond surface into graphite at the points where these two phases enter into contact, a protective carbon coating was applied to iron particles.

In essence, new FPC materials have been herein fabricated by gas pressure assisted liquid metal infiltration of silver and silver-3%silicon alloy into densely packed diamond-iron powder preforms. The thermal conductivity and magnetic permeability are discussed with the help of modelling schemes and scanning electron microscopy that allows a direct access to a close view of the different interfaces. Unfortunately, most of the available literature does not provide enough data and/or information to allow a detailed comparison with the results discussed in this work. In particular, we have not found any reliable work presenting both thermal and magnetic properties of a given material.

2. Materials and Procedures

2.1 Materials

Infiltrations were done with pure Ag 99.9% and Ag-3wt%Si alloy. Pure silver was supplied by Heraeus S.A. (Madrid, Spain). The silver-silicon alloy, in its eutectic composition (Ag-3wt%Si), was prepared in the laboratories of the University of Alicante, in an induction furnace designed for this purpose that works under inert argon atmosphere. The silicon used for the preparation of this alloy was purchased in lumps shape from Goodfellow (Cambridge Limited, England). According to specifications purity is higher than 99,9%.

Diamond particles of different average diameters (225-540 μm) and ISD 1700 quality were purchased from Iljin Diamond Co., Ltd. (Korea). Iron powder (purity >99%) with several average particle diameters (15-400 μm), purchased from Goodfellow (Cambridge Limited, England), was used throughout the experiments. Diamond particles were highly regular both in size and shape while Fe particles had a very irregular shape and a variable size (see Figure 1).

2.2 Coating of iron particles

In order to avoid alloying with the infiltrating metal, iron particles were coated with amorphous carbon by pyrolysis of polyvinylpyrrolidone (PVP) polymer. For that sake, 2g of PVP were dissolved in 60 ml of ethanol under vigorous stirring conditions. Afterwards, iron particles were added to the dissolution and

the stirring was kept for hours. Powder was filtered and dried in a heating muffle at 60ºC. Thereinafter iron particles were subjected to heat treatment ~~at 1000ºC in argon atmosphere~~ in order to achieve pyrolysis of the polymer. The pyrolysis treatment was done in a closed chamber in which two subsequent vacuum-argon purging steps were done. In each step vacuum reached 0.01 mbar and argon was inserted in the chamber up to a pressure of 1 bar. The final vacuum, prior to the heat treatment, was 0.001 mbar. The remaining oxygen in the chamber was not measured as carbon-based samples at high temperatures (at 1000ºC as in the present case) can act as an oxygen getter. So, the trace amounts of oxygen would most probably be consumed in sample combustion. Anyhow, the absence of grooves or rough surfaces in samples containing coated iron particles is an indication of low oxygen contents. Figure 1 shows an iron particle already coated plus an amplification of its surface. Coating significantly decreases the surface roughness (see Figure 1c) of the particles practically eliminating the sharp corners that can be clearly noted in Figure 1b. A detail of the surface shown in Figure 1d reveals the smoothing produced by carbon coatings.

2.3 Liquid metal infiltration

The composites were prepared by gas pressure assisted liquid metal infiltration into densely packed preforms. Mixing of large (small) diamond particles with small (large) iron particles and packing of both mono- and bimodal powders were down mechanically. Graphite crucibles were used as infiltration moulds. An ingot of solid metal was placed on top of the packed preform. Prior to melting, vacuum was applied until a pressure of 0.1 mbar was reached.

Heating was done in an electrical furnace that was set at a very low rate (2ºC/min) until 250ºC to allow for slow desorption of humidity and gas adsorbed on particles surface. Subsequently, heating was continued up to 1075ºC at a rate of approximately 5ºC/min. The maximum temperature was maintained for 20 min. The liquid metal was forced into the preform using inert argon gas at a pressure of approximately 4 MPa. The chamber was kept under pressure until metal was directionally solidified. Finally, the pressure was released and the sample demoulded.

2.4 Characterization of composite materials

Thermal conductivity of composites was measured by means of a relative steady-state (equal-flow) technique, in an experimental set up assembled in our laboratories following the ASTM E1225-04

International Standard (see [14] for a detailed explanation). Sample and reference, in contact across their cross sections, were clamped between a room temperature water-cooled block (reference end) and a block connected to a thermally stabilized hot water bath (sample end). The temperature gradient in the sample was measured, and compared to that in the reference, by means of two thermocouples in each of them. The linearity of the temperature gradient in the reference was measured, by means of a third thermocouple, and was typically within ±1%. Accounting also for uncertainties related to a variety of factors (geometry among others) in the sample and in the reference (diameter after grinding, precise position of the thermocouples, thermal conductivity of the reference, etc.) we estimated the overall uncertainty of the measured thermal conductivities to be within ±5%.

The metal-diamond interfaces were characterized by following a coupled procedure that implies: i) direct access to the interface by a preparative method of electro-etching that preserves any interfacial product [19]; and ii) observation under scanning electron microscopy (S-3000N Hitachi microscopy) immediately after sample preparation.

Measurements of magnetic permeability were carried out with an AC permeameter that was assembled at the laboratories of the University of Alicante. It was designed in accordance with ASTM standard designation A772-80. The primary winding was excited with a triangular wave with the help of a function generator. An oscilloscope connected to a data acquisition system measured the voltage induced in the secondary winding. The relative magnetic permeability values were obtained by comparing the voltage induced in the secondary winding of composite sample with a reference sample (Fe 99,99%, purchased from Goodfellow Metals, Cambridge, UK).

3. Particle volume fraction of compacts and composites microstructure

3.1 Particle volume fraction

Experimental data for particle volume fraction V_p in mono-modal (iron or diamond compacts) are reported in Table 2 while those for bimodal mixtures of Fe and diamond particles are shown in Figure 2 and Table 3. Monomodal compacts of diamond particles reached a rather high volume fraction due to their regularity (for comparison, compacts of highly regular SiC particles has at most V_p=0.59, see [20,21,22]). Instead, Fe compacts had a much lower particle volume fraction surely due to their irregular shape and highly rough surface.

V_p for each component in iron/diamond mixtures is given in Table 3. Figure 2 in turn shows calculated (see below) curves of constant particle volume fraction using as variables the fraction of one of the particles plus its average size divided by the other particle size. Data for the following mixtures are shown: a) Diamond-iron mixtures obtained with 400 diamond particles and Fe of several sizes, and, (b) Fe-diamond mixtures containing Fe particles of 400 μm average diameter and diamond particles of several sizes (see Table 1). Experimental values are shown in bold characters. Total volume fraction always increases with the size ratio (see Ref. [20,22]) albeit it reaches the highest values for low contents of iron particles.

The results shown in Figure 2 were obtained by means of Yu and Standish's model [23] for mixtures of two types of particles of any average size ratio. This scheme has proven to accurately reproduce various sets of experimental data [23,24,25],

$$\left(\frac{v - v_l x_l}{v_s}\right)^2 + 2G\left(\frac{v - v_l x_l}{v_s}\right)\left(\frac{v - x_l - v_s x_s}{v_l - 1}\right) + \left(\frac{v - x_l - v_s x_s}{v_l - 1}\right)^2 = 1 \qquad (1)$$

where *v* is the apparent volume occupied by unit solid volume of particles (i.e., the reciprocal of the particle packing volume fraction V) and *x* is the fraction of an inclusion type in the bimodal particle mixture. The subscripts *l* and *s* refer to large (or "coarse") and small particles, respectively. The parameter G is related to the particle size ratio; G can be calculated using the following (slightly rewritten) empirical formula [25],

$$G = 1 - (1 - v_l)^{0.63}\left(\frac{v_l}{v_s - v_l v_s}\right)^{-0.63} + \left(\frac{1}{R}\right)^{-1.89} \qquad (2)$$

where R is the ratio of coarse-to-small particle radii.

3.2 Composites microstructure

Figure 3 illustrates the characteristic microstructure of the composites fabricated in this work. Ag/diamond composites (Fig. 3a) show a rather "clean" microstructure. Adding 3wt% Si produces a much rougher landscape due to the formation of the AgSi eutectic. Ag/diamond-iron composites are relatively free of precipitates or intermetallics, though those present are rather large (see Figures 3c and

3d). They probably are compounds of FeC formed under a low nucleation rate and a significantly larger growth rate. Replacing pure silver by the AgSi eutectic alloy sharply increases nucleation rate. Diamond particles are now full of little holes that are likely originated through etching of FeCSi particles. Holes are also observed in zones of the AgSi-Fe particles mixture (see Figure 3f). This indicates that formation of FeCSi is probably nucleated on the AgSi eutectic (see Figure 3b). These holes are no longer observed when carbon coated Fe particles are used to fabricate the composite. Instead, Fe particles and the AgSi eutectic are cleanly identified (see Figures 3g and 3h).

4. Results and discussion

4.1 Composites with inclusions of either diamond or iron particles with and without carbon coating

Monomodal composites are considered here not only for comparison with the bimodal composites proposed in the present work, but also because the experimental data for their TC allow to derive the interface thermal conductance h_i at the six relevant interfaces, namely, Ag/diamond, AgSi/diamond, Ag/Fe, Ag/Fe$_c$, AgSi/Fe and Ag/Fe$_c$. Experimental results for the TC and the relative magnetic permeability of the mono-modal composites investigated in this work are reported in Table 2. Data for TC, in combination with the semi-empirical theory described below, allow deriving h_i for each interface (see Figure 4 and Table 2).

The thermal conductivity of composite materials can be predicted with the Generalized Differential Effective Medium Scheme (GDEMS). This scheme has been successfully applied to model thermal conduction in different composite materials [16,26,27]. The leading integral equation of the GDEMS approach for the TC of a multi-phase composite material is,

$$\int_{\kappa_m}^{\kappa_c} \frac{d\kappa}{\kappa \sum_i x_i \frac{\left(\kappa_i^{eff} - \kappa\right)}{\left(\kappa - \kappa_i^{eff}\right)P_i - \kappa}} = -ln(1 - V) \qquad (3)$$

where κ is the thermal conductivity and the subscripts *c* and *m* refer to composite and matrix, respectively. x_i is the fraction of inclusion *i* in the total amount of inclusions of the composite (hence, $\Sigma_i x_i$=1), *V* is the total volume fraction of inclusions and P_i is the polarization factor of inclusion *i* (equal to 0,33 for spheres, as modelled in this study). κ_i^{eff} is the effective thermal conductivity of inclusion i, which

is, for spherical geometries, related to its intrinsic thermal conductivity, κ_i^{in}, the matrix/inclusion interface thermal conductance h_i, and the radius of the inclusion r_i, by

$$\kappa_i^{eff} = \frac{\kappa_i^{in}}{1 + \frac{\kappa_i^{in}}{h_i\, r_i}} \tag{4}$$

In general, the integral on the left hand side of Eq. (3) has no analytical solution so that Eq. (3) needs to be solved numerically with the appropriate mathematical software.

The numerical results for the TC of monomodal composites of either Ag or AgSi with diamond, Fe and carbon-coated Fe particles are depicted in Figure 4. The fittings, that were done with a single parameter, namely, the interface thermal conductance *h*, are rather satisfactory. The high relevancy of *h* has been highlighted already by many authors [28-33]. In the case of AgSi/diamond, the fitted *h* is similar to that reported in Ref. [16]. *h* for Ag/diamond is almost 1.5 orders of magnitude smaller than that for Ag/Fe (see Table 2). Adding Si substantially increases *h* in composites containing diamond and only slightly in those which contain uncoated Fe. AgSi/Fe shows the largest *h*. The smallest *h* is that corresponding to Ag/diamond and all composites containing carbon-coated iron (all three are actually very similar).

It is interesting to comment some general trends followed by the experimental data for TC reported in Table 2. Silicon alloying sharply increases the TC of diamond composites, whereas it decreases, albeit to a much less extent, the TC of both uncoated and coated Fe composites, being this decrease larger in the latter. In the case of diamond composites the origin of this behaviour is the increase in wetting at the interface promoted by Si (note also the factor of 40 increase in *h*). This is better understood by rewriting Eq. (4) in the cases that the parameter $x_i = \kappa_i^{in}/(h_i r_i)$ which controls the change in TC of particles due to thermal mismatch, is either much greater or much smaller than 1, namely,

$$\kappa_i^{eff} \sim \frac{\kappa_i^{in}}{x_i} = h_i r_i \quad for\ \ x_i \gg 1 \tag{5a}$$

$$\kappa_i^{eff} \sim \kappa_i^{in}(1 - x_i) \quad for\ \ x_i \ll 1 \tag{5b}$$

These approximate expressions are very revealing. While for $x_i >> 1$ the effective TC of particles does not depend on their intrinsic TC, for $x_i << 1$ the two magnitudes are related linearly. For $x_i >> 1$ the effective TC is proportional to the particle size and the interface thermal conductance.

This allows a deeper discussion of the experimental data for the TC of composites, a magnitude directly related to the effective TC of the components. Ag/diamond composites have x_i in the range 6.64-3.9 (from larger to smaller particles) and, thus, Eq. (5a) leads to significantly smaller TC than those derived from Eq. (5b) for AgSi/diamond composites with x_i varying in the range 0.16-0.09 and, thus, an effective TC directly proportional to the high intrinsic TC of diamond. This also explains the much larger decrease as the particle size decreases in the TC of Ag/diamond (25% decrease) as compared to AgSi/diamond (10% decrease), as in the former case the effective TC is proportional to the particles average radii.

The parameter x_i in Ag/Fe and AgSi/Fe composites varies, as size decreases, in the range 0.005-0.07 and 0.002-0.024, respectively. Eq. (5b) then leads, for both composites, to an effective TC that does not vary appreciably with particle size. In addition, although AgSi/Fe has a higher *h* three times that of Ag/Fe, the likely increase in TC that this should promote is overcompensated by the decrease caused by Si dissolution in the Ag matrix. In the case of coated Fe particles, however, x_i varies in the ranges 0.22-2.6 and 0.18-2.4 for Ag/Fe_c and AgSi/Fe_c, respectively. This implies, for the largest particles Fe1, a slight decrease in TC with respect to uncoated Fe, and a substantially larger decrease in TC with size, as particles Fe2 and Fe3 are much smaller than Fe1 (note that in Fe2 and Fe3 the effective TC is approximately proportional to particle size, see Eq. (5a)).

As regards magnetic permeability (relative to that of high purity iron), it is noted that both, Si alloying and carbon coating of Fe particles, produce an overall slight increase of permeability. Anyhow, all composites investigated here containing Fe as a single reinforcement, show a relative magnetic permeability higher than 0.35, that is, not much smaller than the maximum possible that coincides with the volume fraction of Fe particles (0.48).

4.2 - Composites with bimodal inclusions of diamond and iron particles with and without carbon coating

Experimental results for the TC and the relative magnetic permeability of the bimodal composites investigated in this work are reported in Table 3 and Figures 5, 6 and 7. In order to check the accuracy and, thus, the validity of the GDEMS approach in predicting the TC of the present bimodal composites, we have first plotted in Figure 5 the calculated versus the experimental values of the TC. The GDEMS

approach incorporates the values of the interface thermal conductance *h* at the six interfaces present in these composites, derived from data for the mono-modal composites. The straight line included in Figure 5 means "perfect agreement". The plot clearly indicates the validity of the GDEMS approach to predict the TC of the bimodal composites investigated here and, consequently, to elaborate the useful curves of constant TC. Figure 6 shows the curves of constant thermal conductivity for composites fabricated with either Ag or AgSi, and either the largest diamond particle with iron particles of several sizes or the largest iron particles with diamond particles of several sizes. These curves are highly useful in designing a composite for a given application requiring prescribed properties (see next subsection).

Some obvious features, and others that are not so apparent, characterize the results shown in Table 3, namely: i) The TC increases with the content of diamond particles, while the relative magnetic permeability increases with iron content (see Table 3 and Figure 7). ii) Si addition to A1 and A2 (large diamond and large uncoated iron particles) notably increase TC but does not affect much the magnetic permeability (see B1 and B2 in Table 3); this is a consequence of the increase in wetting promoted by Si (see Table 2) that only affects TC. iii) Decreasing the size of iron particles (see B3 and B4 of Table 3) affects only slightly the properties (changes approximately in the range 10-20%) that, in addition, are obscured by small differences in particle contents. iv) Replacing uncoated by carbon-coated iron in Ag based composites, increases TC in a factor of two, while the magnetic permeability increases in a 50% only in the case of iron particles volume fractions higher than 0.4; This is probably due to the decrease of reactions between diamond and Fe (to produce FeC or, more likely Fe_3C) promoted by the thin C coating. v) Similar effects are observed in AgSi based composites.

4.3 Selection of materials for electric conversion applications

Although some of the mono-modal Ag/Fe or Ag-Si/Fe composites have sufficiently high thermal conductivity (> 200 W/mK) and relative magnetic permeability (> 0.3) they may have an excessively high linear thermal expansion coefficient α_c. A reasonable estimation of the CTE can be obtained by means of the linear mixture rule. According to this rule α_c can be written as,

$$\alpha_c = \sum_{i=1}^{N} V_i \alpha_i \qquad (5)$$

where N is the number of components each of them having a volume fraction of V_i and a linear thermal expansion coefficient α_i. As reported in the literature, diamond, iron, Ag and Ag-3wt%Si have CTE of 1, 12, 19 and 17 ppm/K. Inserting these values in Eq. (5) we obtain 15.6 and 14.6 ppm/K for Ag/Fe and Ag-Si/Fe composites. Similarly, the CTE of bimodal composites can be calculated. The results are reported in Table 3. The lowest CTE (6.8 ppm/K) correspond to the composites containing the highest volume fraction of large diamond particles (0.59). This value is substantially higher than those obtained with mono-modal composites. It is likely that there are applications for which the CTE attained with a volume fraction of 0.47, namely, 9.7 ppm/K may be enough.

Figs. 3-7 and Tables 1 and 2 may be of great help in choosing a composite for a particular application. For instance, if a relative magnetic permeability of 0.1 suffices, a composite like B4´ will do the job with no problems. If the CTE of B4´ is too low, the volume fraction of diamond particles can be reduced (the TC is high enough to allow a considerable reduction of diamond particles) without changing, or even increasing, the volume fraction of Fe particles. If a higher relative magnetic permeability is required (say, for instance, 0.30) the contents of B4´ can be varied as follows: the volume fraction of Fe particles raised up to 0.30 and that of diamond particles decreased to 0.45 (this does not change the total particle volume fraction around 0.75). This composite should have a CTE around 10 ppm/K and a TC close to 500 W/mK.

5. Concluding Remarks

This work was addressed to investigate whether any composite containing a metallic alloy and magnetic particles may fit the specifications of electric conversion applications. These applications require sufficiently high magnetic permeability and thermal conductance and a low (adjustable) thermal expansion coefficient. Guided by both chemical and physical considerations, it was decided to investigate composites fabricated by gas pressure infiltration of Ag or Ag-3wt%Si alloys into compacts of bimodal mixtures of diamond (high thermal conductivity) and iron particles (high magnetic permeability). The rather extensive study carried out allow to conclude that materials containing volume fractions of *large* diamond particles (V_D = 0.4-0.6), carbon-coated *small* Fe particles (V_{Fe} = 0.1-0.3) and Ag-3wt%Si *eutectic* alloy, show the following attractive properties: a TC = 300-500 W/mK**,** a relative magnetic permeability within the range 0.1-0.3, and a CTE = 7-10 ppm/K. These properties fit the specifications of most electric conversion applications.

Acknowledgements

The authors acknowledge partial financial support from "Ministerio de Ciencia e Innovación" (grant MAT2016-77742-C2-2-P).

References

[1] Gutfleisch O, Willard MA, Brück E, Chen CH, Sankar SG, Ping Liu J. Magnetic Materials and Devices for the 21st Century: Stronger, Lighter, and More Energy Effi cient. Adv. Mater. 23 (2011): 821–842.

[2] Amadori S, Bonetti E, Campari EG, Pasquini L. Production and Characterization of Aluminum Iron Powder Composites with Ferromagnetic Properties. Mater Sci Forum 2011; 678: 135–143.

[3] Hamlera A, Goricˇan V, Sˇ usˇtarsˇicˇ B, Sirc A. The use of soft magnetic composite materials in synchronous electric motor. Journal of Magnetism and Magnetic Materials. 2006; 304: e816–e819.

[4] Okimoto K, Satoh T, Horiishi N. Fabrication of a Magnetic Composite Material from Zn-22Al Superplastic Powder. J Japan Soc Powder & Powder Metallurgy. 1988; 35(2): 47-52.

[5] Shokrollahi H, Janghorban K. Soft magnetic composite materials (SMCs). Journal of Materials Processing Technology. 2007; 189: 1–12.

[6] Okimoto K, Satoh T, Matsuyama H, Oka M. Fabrication of a Magnetic Composite Material from Zn-22Al Base Superplastic Powder (2nd Report). J. Japan Soc. Powder & Powder Metallurgy. 1991; 38(5): 673-680.

[7] Shin K, Wong CR, Whang SH. Fabrication and damping capacity of Cu-Zn-Al composites processed by powder metallurgy route. Mater Sci & Eng A - Struct Mater: Properties, Microstructure & Processing. 1993; A165: 35-43.

[8] Schalek RL, Leslie-Pelecky DL, Knight J, Sellmyer DJ, Axtell SC. Tailoring of the magnetic properties of $SmCo_5$:$Nb_{0.33}Cr_{0.67}$ nanocomposites using mechanical alloying. IEEE Transactions on Magnetics 1995; 31(6): 3772-3774.

[9] Yamamoto TA, Nishimaki K, Harabe T, Shiomi K, Nakagawa T, Katsura M. Magnetic composites composed of iron-nitride nanograins dispersed in a silver matrix. Nanostructured Mater. 1999; 12(1): 523-526.

[10] Nakayama T, Yamamoto TA, Choa YH, Niihara K. Structure and magnetic properties of iron oxide dispersed silver based nanocluster composite. J Mater Sci. 2000; 35(15): 3857-3861.

[11] Franco V, Batlle X, Labarta A. J Magnetism & Magnetic Mater. CoFe-based granular alloys: the role of the metallic matrix. 2000; 210(1-3): 295-301.

[12] Borgohain C, Acharyya K, Sarma S, Senapati KK, Sarma KC, Phukan P. A new aluminum-based metal matrix composite reinforced with cobalt ferrite magnetic nanoparticle. J Mater Sci. 2012; 48(1): 162–171.

[13] Borgohain C, Senapati KK, Mishra D, Sarma KC, Phukan P. A new CoFe(2)O(4)-Cr(2)O(3)-SiO(2) fluorescent magnetic nanocomposite. Nanoscale 2010; 2(10): 2250–2256.

[14] Shigeyoshi Y, Mitsuraru S, Norihiko O. US patent, US6,962,753 B1, 1996.

[15] Wan M, Fan J. Synthesis and ferromagnetic properties of composites of a water-soluble polyaniline copolymer containing iron oxide. J Polym Sci A Polym Chem. 1998; 36(15): 2749-2755.

[16] Weber, L, Tavangar, R. Diamond-Based Metal Matrix Composites for Thermal Management Made by Liquid Metal Infiltration: Potential and Limits. Adv Mater Res 2009; 59: 111–115.

[17] Monje IE, Louis E, Molina JM. On critical aspects of infiltrated Al/diamond composites for thermal management: Diamond quality versus processing conditions. Composites: Part A 2014; 67: 70–76.

[18] Gale WF, Totemeier TC (Eds). Smithells Metals Reference Book, 8th ed. Elsevier. 2004.

[19] Monje IE, Louis E, Molina JM. Aluminum/diamond composites: A preparative method to characterize reactivity and selectivity at the interface. Scr Mater. 2012; 66(10): 789–792.

[20] Molina JM, Piñero E, Narciso J, García-Cordovilla C, Louis E. Liquid metal infiltration into ceramic particle preforms with bimodal size distributions. Curr Opin Solid State Mater 2005; 9:202–210.

[21] García-Cordovilla C, Louis E, Narciso J. Pressure infiltration of packed ceramic particles by liquid metals. Acta Mater 1999; 47:4461–4479.

[22] Molina JM, Saravanan RA, Arpón R, García-Cordovilla C, Louis E, Narciso J. Pressure infiltration of liquid aluminium into packed SiC particulate with a bimodal size distribution. Acta Mater 2002; 50:247–57.

[23] Yu AB, Standish N. An analytical–parametric theory of the random packing of spheres. Powder Technol 1988; 55:171–86.

[24] Yu AB, Zhou RP. Prediction of the porosity of particle mixtures: a review. Kona Powder Part 1998; 16:68–81.

[25] Finkers HJ, Hoffmann AC. Structural ratio for predicting the voidage of binary particle mixtures. AIChE J 1998; 44:495–7.

[26] Molina JM, Rhême M, Carron J, Weber L. Thermal conductivity of aluminum matrix composites reinforced with mixtures of diamond and SiC particles. Scr Mater. 2008; 58(5): 393–396.

[27] Tavangar R, Molina JM, Weber L. Assessing predictive schemes for thermal conductivity against diamond-reinforced silver matrix composites at intermediate phase contrast. Scr Mater. 2007; 56(5) 357–360.

[28] Monachon C, Weber L. Thermal boundary conductance between refractory metal carbides and diamond. Acta Mater. 2014; 73: 337–346.

[29] Prieto R, Molina JM, Narciso J, Louis E. Fabrication and properties of graphite flakes/metal composites for thermal management applications. Scr Mater. 2008; 59, (1): 11–14.

[30] Prieto R, Molina JM, Narciso J, Louis E. Thermal conductivity of graphite flakes–SiC particles/metal composites. Compos. Part A Appl Sci Manuf 2011; 42 (12): 1970–1977.

[31] Monje IE, Louis E, Molina JM. Optimizing thermal conductivity in gas-pressure infiltrated aluminum/diamond composites by precise processing control. Compos. Part A Appl. Sci. Manuf. 2013; 48: 9–14.

[32] Kida M, Weber L, Monachon C, Mortensen A. Thermal conductivity and interfacial conductance of AlN particle reinforced metal matrix composites. J. Appl. Phys. 2011; 109(6): 064907.

[33] Yang W, Peng K, Zhu J, Li JD, Zhou L. Enhanced thermal conductivity and stability of diamond/aluminum composite by introduction of carbide interface layer. Diam Relat Mater. 2014; 46: 35–41.

Tables legend

Table 1. *Thermal conductivity (in W/mK) of Ag and Ag-3wt%Si and the iron and diamond particles used in this work to fabricate the composites. Average values of particle diameter (in μm) and codes assigned to each material are also shown.*

***Table 2**. Experimental results for the thermal conductivity TC (W/mK) and the relative magnetic permeability μ_r of composites with mono-modal inclusions of either iron (with Fe_c or without carbon-coating) or diamond particles (codes for particles are given in Table 1). h stands for the interface thermal conductance (in $W/m^2.K$) fitted to the experimental data for TC (see text).*

***Table 3** Experimental results for the thermal conductivity TC (W/mK), the coefficient of thermal expansion α (in ppm/K) and the relative magnetic permeability μ_r of composites with bimodal mixtures of iron (either with Fe_c or without carbon-coating) and diamond particles (codes for particles are given in Table 1). The volume fraction of each particle type is given separately (note that the metal volume fraction is given by $V_m = 1-V_D-V_{Fe}$).*

Figures legend

Figure 1. *Depicts SEM micrographs of: a) diamond particles ISD 1700 40/50 with 395 μm of average diameter, and, b) as-supplied iron particles with average particle diameter of 60 μm; c) and d) carbon coated Fe particles.*

Figure 2. SEM microstructures of the following composites: a) Ag/diamond, b) AgSi/diamond, c) and d) Ag/diamond-iron, e) and f) AgSi/diamond-iron; g) and h) AgSi/diamond-carbon-coated Fe composites.

Figure 3 – Calculated curves of constant particle volume fraction for: a) Diamond-iron mixtures obtained with 400 diamond particles and Fe of several sizes, and, (b) Fe-diamond mixtures containing Fe particles of 400 μm average diameter and diamond particles of several sizes (see Table 1). Experimental values are shown in bold characters.

Figure 4. Experimental results (filled and empty symbols) for the thermal conductivity of composites of either pure Ag or AgSi alloy and diamond (a), Fe (b) or carbon-coated Fe particles (c), versus the logarithm of the particle diameter. Broken lines are fittings of the experimental data by means of GDEMS (see Eq. (3)). The resulting matrix/inclusion interface thermal conductance h (in $W/m^2.K$) derived from the fittings is given as insets in the Figures.

Figure 5. Calculated versus experimental thermal conductivities in composites with bimodal mixtures of diamond-Fe particles with (filled symbols) and without (empty symbols) carbon coating. Either Ag or AgSi was used as host metal (see Table 3).

Figure 6. Curves of constant thermal conductivity (in W/mK) for composites containing: a) and c) diamond-iron mixtures obtained with 395 μm diamond particles and Fe of several sizes, and, (b) and d) Fe-diamond mixtures containing Fe particles of 398 μm average diameter and diamond particles of several sizes (see Table 1); in a) and b) Ag was the host metal whereas in c) and d) the alloy AgSi was used. See Table 3.

Figure 7. Experimental relative magnetic permeability depicted versus the volume fraction of Fe particles in composites with bimodal mixtures of large diamond particles (D1 in Table 1) and small (Fe3) or large (Fe1) iron particles with (black filled circles) and without (red empty triangles) carbon coating. Either Ag or AgSi was used as host metal (see Table 3).

Tables

Table 1. *Thermal conductivity (in W/mK) of Ag and Ag-3wt%Si and the iron and diamond particles used in this work to fabricate the composites. Average values of particle diameter (in μm) and codes assigned to each material are also shown.*

Code	***Material***	***Average size***	***TC***
Ag	Ag	-	420
AgSi	Ag-3wt.%Si	-	240 (as cast) 330 (after heat treatment)
D1	ISD1700 40/50	395	1608 [17]
D2	ISD1700 50/60	285	
D3	ISD1700 60/80	230	
Fe1	Fe 380-420	398	80 [18]
Fe2	Fe 38-45	42	
Fe3	Fe 20-38	30	

Table 2. *Experimental results for the thermal conductivity TC (W/mK) and the relative magnetic permeability μ_r of composites with mono-modal inclusions of either iron (with* Fe_c *or without carbon-coating) or diamond particles (codes for particles are given in Table 1). h stands for the interface thermal conductance (in W/m^2.K) fitted to the experimental data for TC (see text).*

Material	V_D	V_{Fe}	***TC***	***h***	μ_r
Ag/D1	0.62	-	260	1.05e+06	-
Ag/D2			208		
Ag/D3			197		
AgSi/D1			825	4.3e+07	
AgSi/D2			766		
AgSi/D3			743		
Ag/Fe1	-	0.48	223	3.74e+07	0.36
Ag/Fe2			218		0.39
Ag/Fe3			216		0.37
AgSi/Fe1			188	1.1e+08	0.41
AgSi/Fe2			185		0.38
AgSi/Fe3			184		0.43
Ag/Fe_c1			213	1.0e+06	0.41
Ag/Fe_c2			175		0.38
Ag/Fe_c3			170		0.42
AgSi/Fe_c1			172	1.2e+06	0.37
AgSi/Fe_c2			140		0.41
AgSi/Fe_c3			135		0.43

Table 3 *Experimental results for the thermal conductivity TC (W/mK), the coefficient of thermal expansion* α *(in ppm/K) and the relative magnetic permeability* μ_r *of composites with bimodal mixtures of iron (either with* Fe_c *or without carbon-coating) and diamond particles (codes for particles are given in Table 1). The volume fraction of each particle type is given separately (note that the metal volume fraction is given by* $V_m = 1-V_D-V_{Fe}$*).*

Code	***Material***	V_D	V_{Fe}	***TC***	μ_r	α
A1	Ag/(D1+Fe1)	0.10	0.40	88	0.23	14.4
A2	Ag/(D1+Fe1)	0.47	0.12	118	0.11	9.7
B1	AgSi/(D1+Fe1)	0.10	0.40	105	0.18	13.4
B2	AgSi/(D1+Fe1)	0.47	0.12	402	0.11	9.7
B3	AgSi/(D1+Fe3)	0.11	0.43	97	0.24	13.1
B4	AgSi/(D1+Fe3)	0.59	0.15	308	0.07	6.8
A1´	Ag/(D1+Fe_c1)	0.10	0.40	220	0.34	13.4
A2´	Ag/(D1+Fe_c1)	0.47	0.12	227	0.10	9.7
B1´	AgSi/(D1+Fe_c1)	0.10	0.40	218	0.38	13.4
B2´	AgSi/(D1+Fe_c1)	0.47	0.12	587	0.11	9.7
B3´	AgSi/(D1+Fe_c3)	0.11	0.43	203	0.40	13.1
B4´	AgSi/(D1+Fe_c3)	0.59	0.15	668	0.13	6.8

Figures

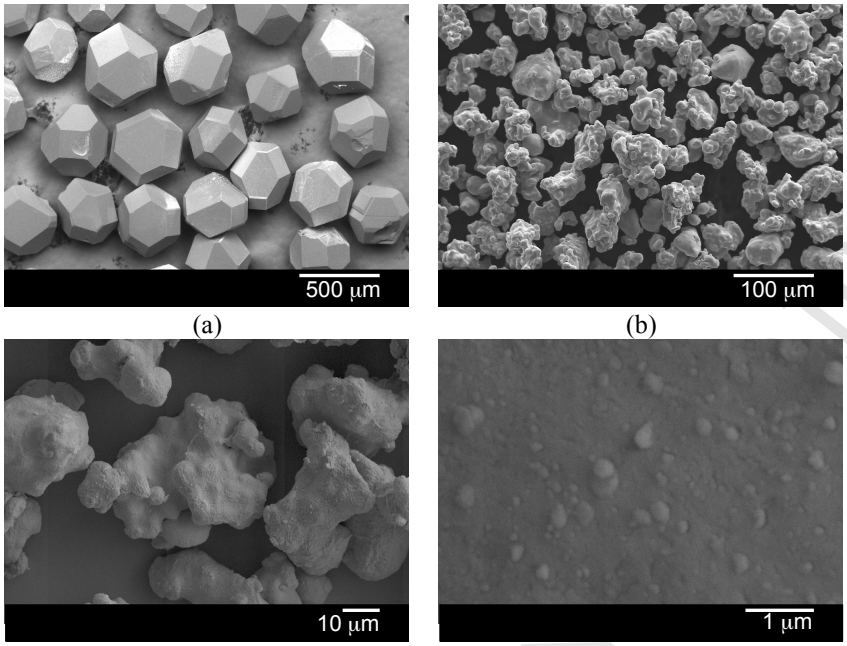

Figure 1

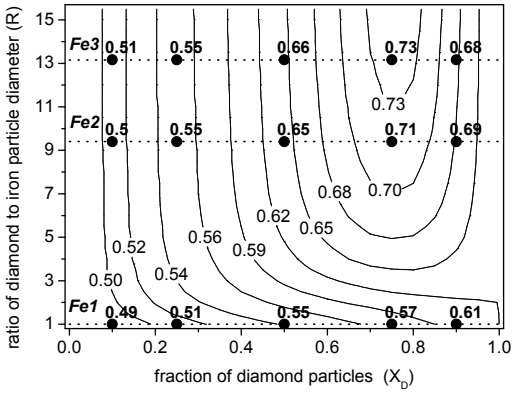

(a)

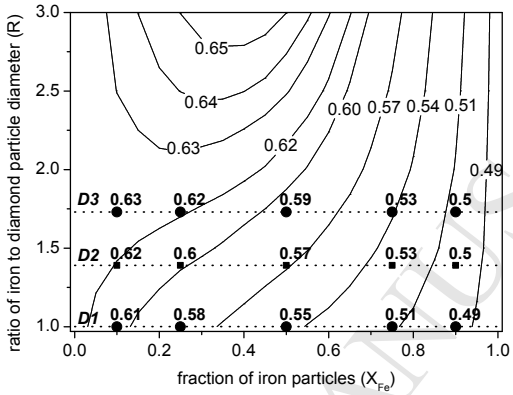

(b)

Figure 2

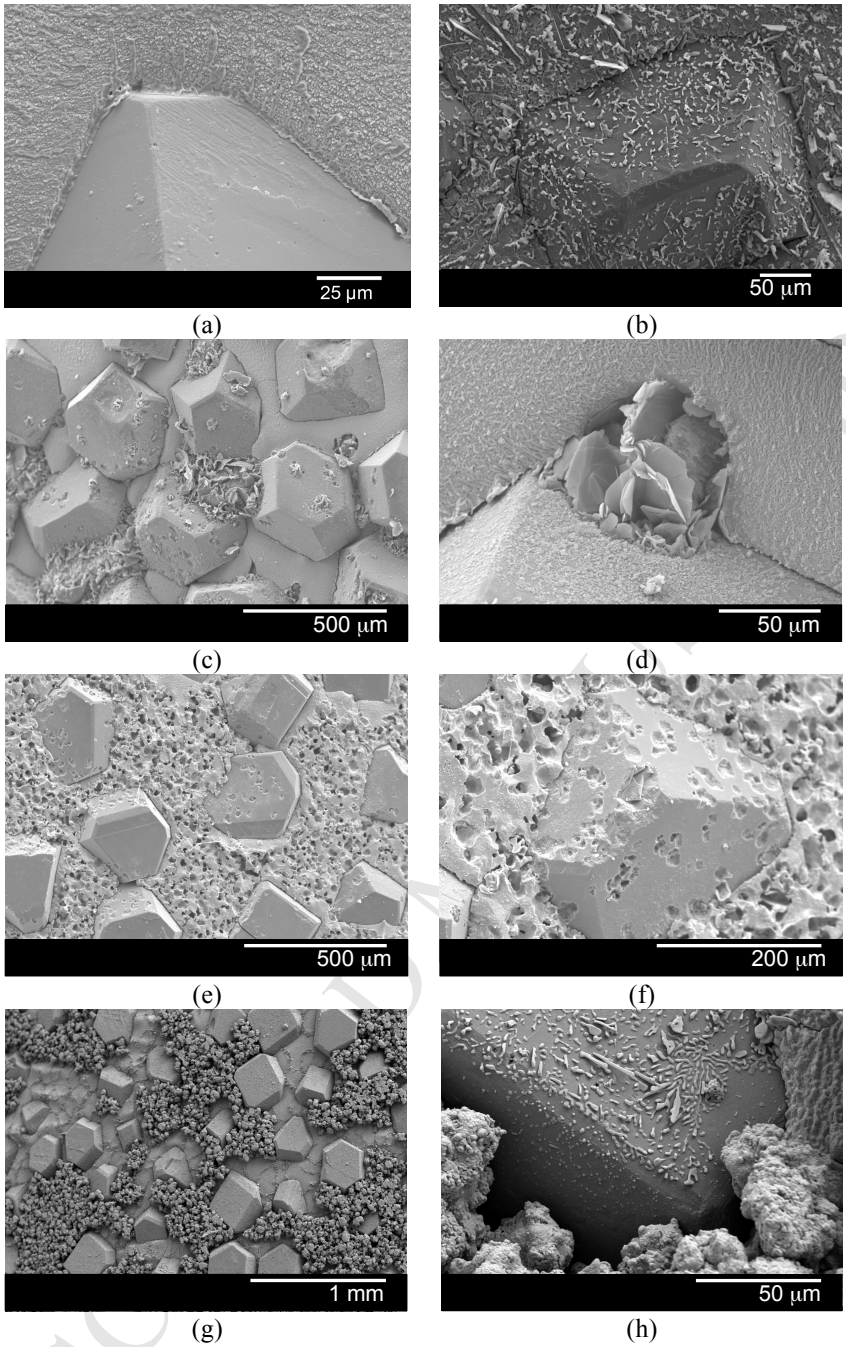

Figure 3

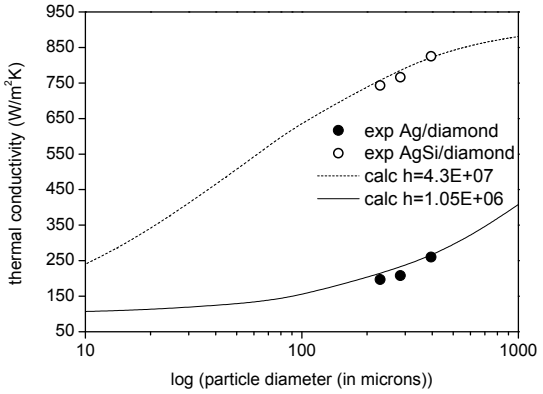

(a)

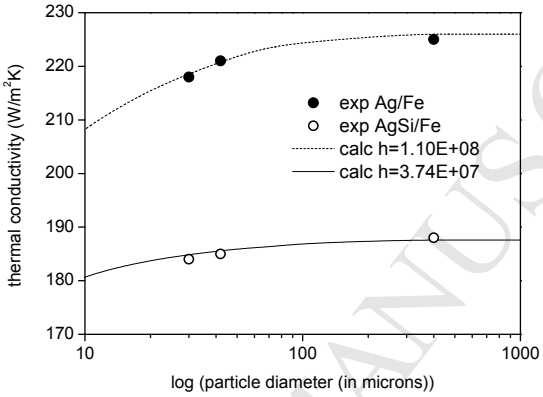

(b)

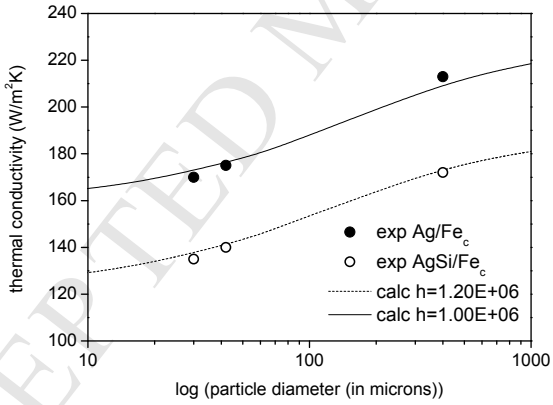

(c)

Figure 4

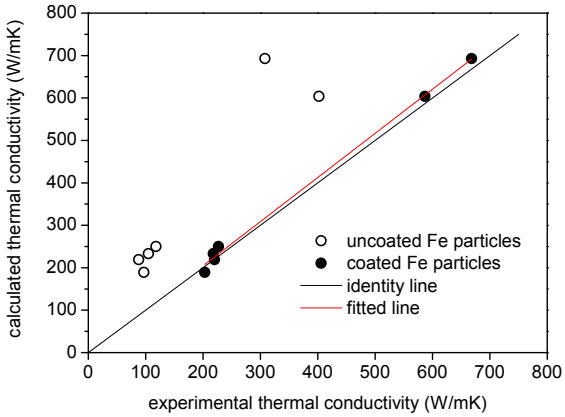

Figure 5

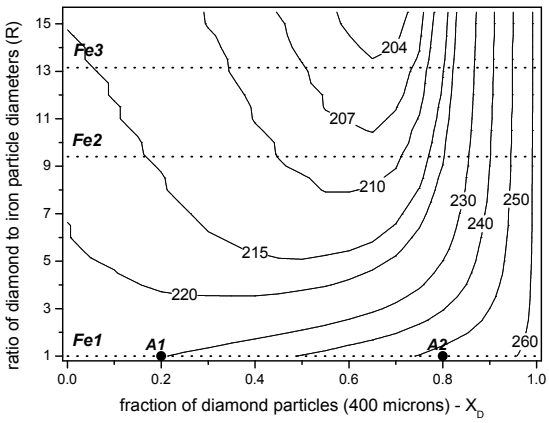

(a)

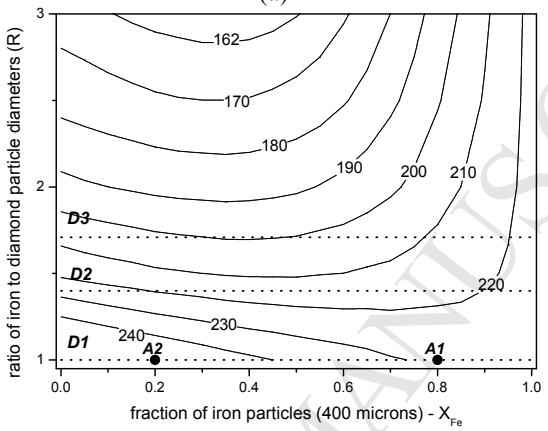

(b)

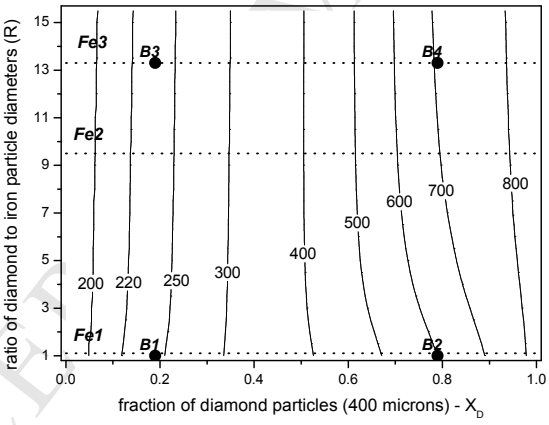

(c)

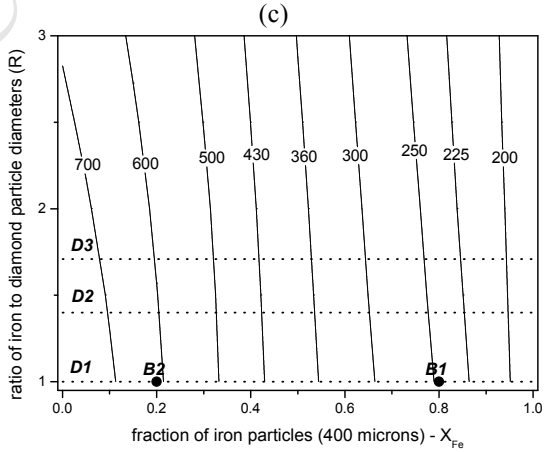

(d)

Figure 6

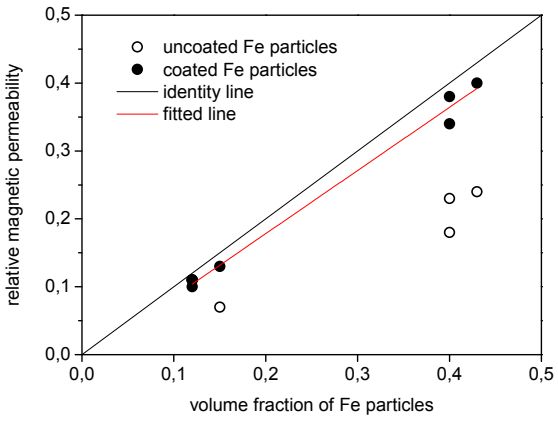

Figure 7

Highlights

- Fe-diamond/Ag and Fe-diamond/AgSi composites are fabricated by metal infiltration
- Fe and diamond particles undergo detrimental solid-solid reactions during processing
- Interface engineering by carbon coating of Fe particles (Fe_C) is followed
- Carbon coating sharply decreases the Ag-Fe and AgSi-Fe interface thermal conductance
- Fe_C (>40%)–diamond/Ag-Si composites are adequate for electric conversion applications